Changements de l'hydrologie et de la circulation: l'exemple de l'Atlantique Nord

H. Mercier

Laboratoire de Physique des Océans

Ifremer

CNRS INSU Observer & comprendre

université de bretagne occidentale

Le transport de chaleur océanique

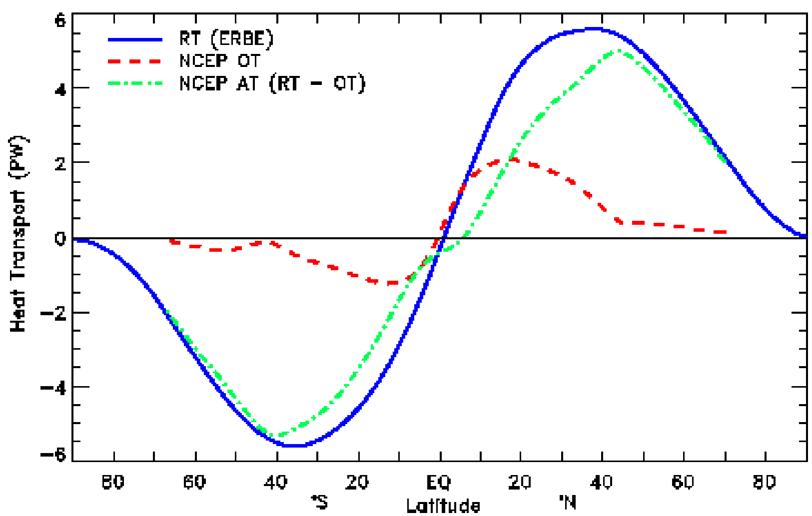

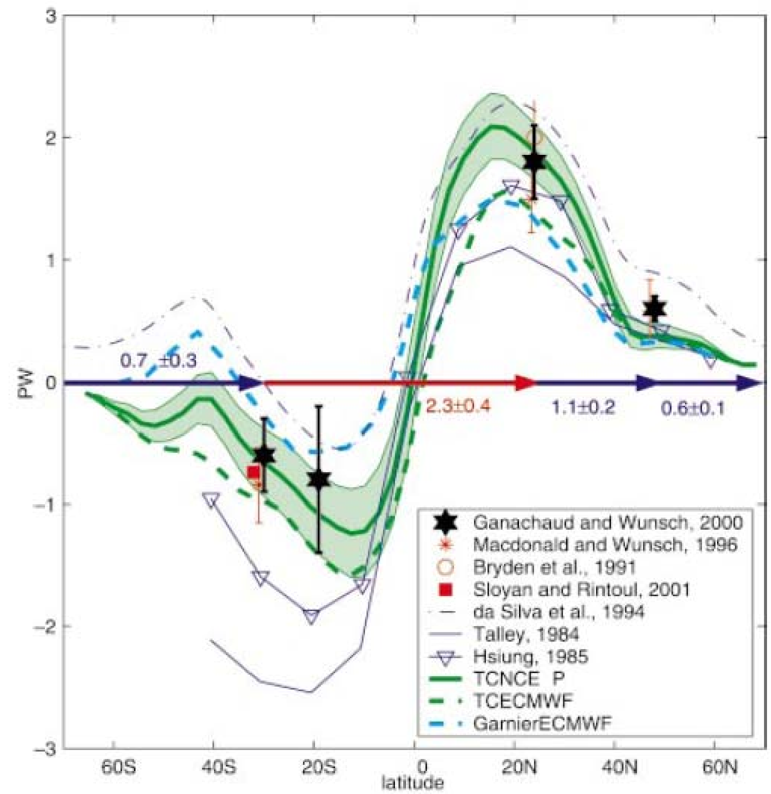

(positif vers le nord)

Trenberth and Caron (2001) Ganachaud and Wunsch (2000)

Transport méridien de chaleur (Talley, 2003)

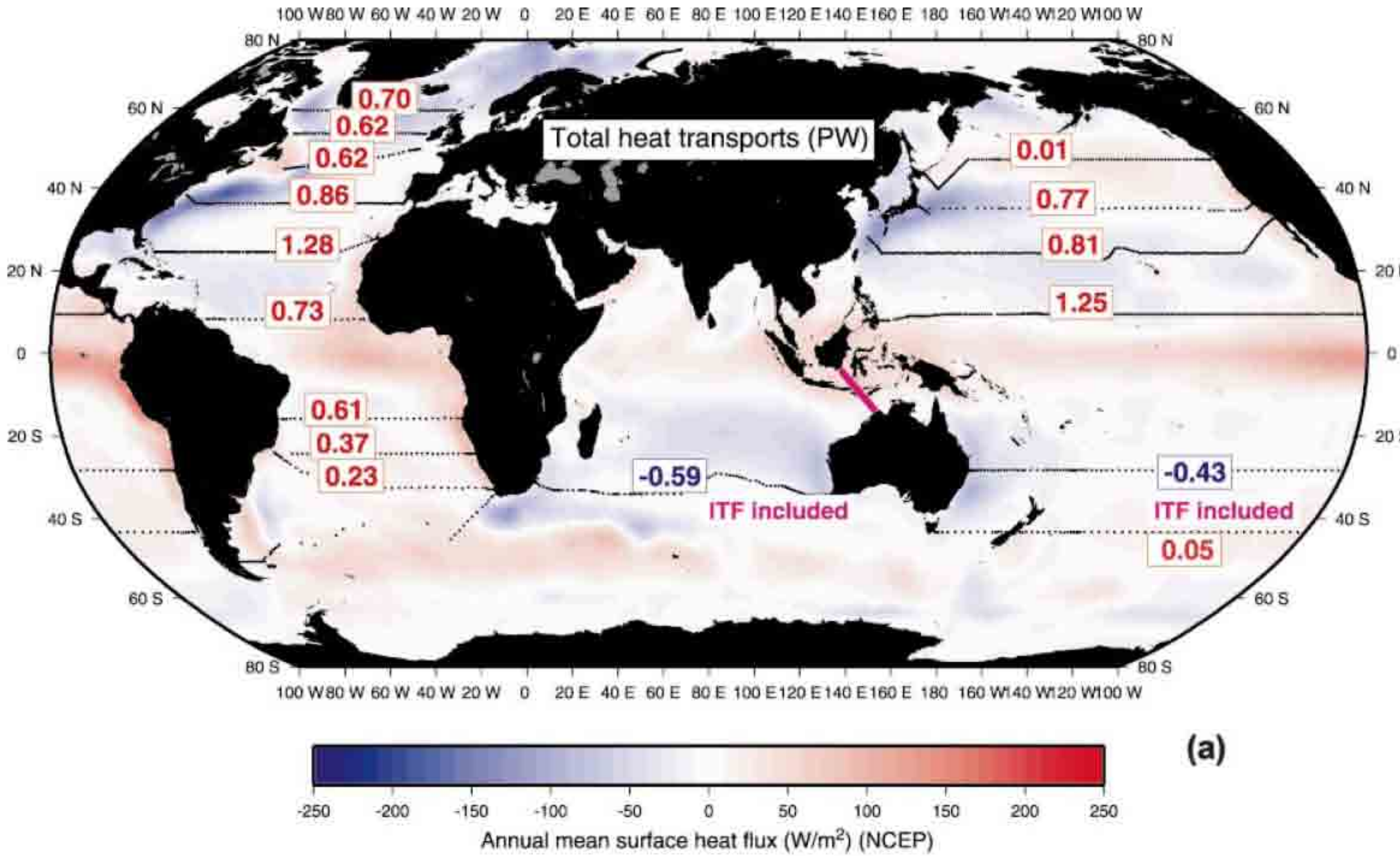

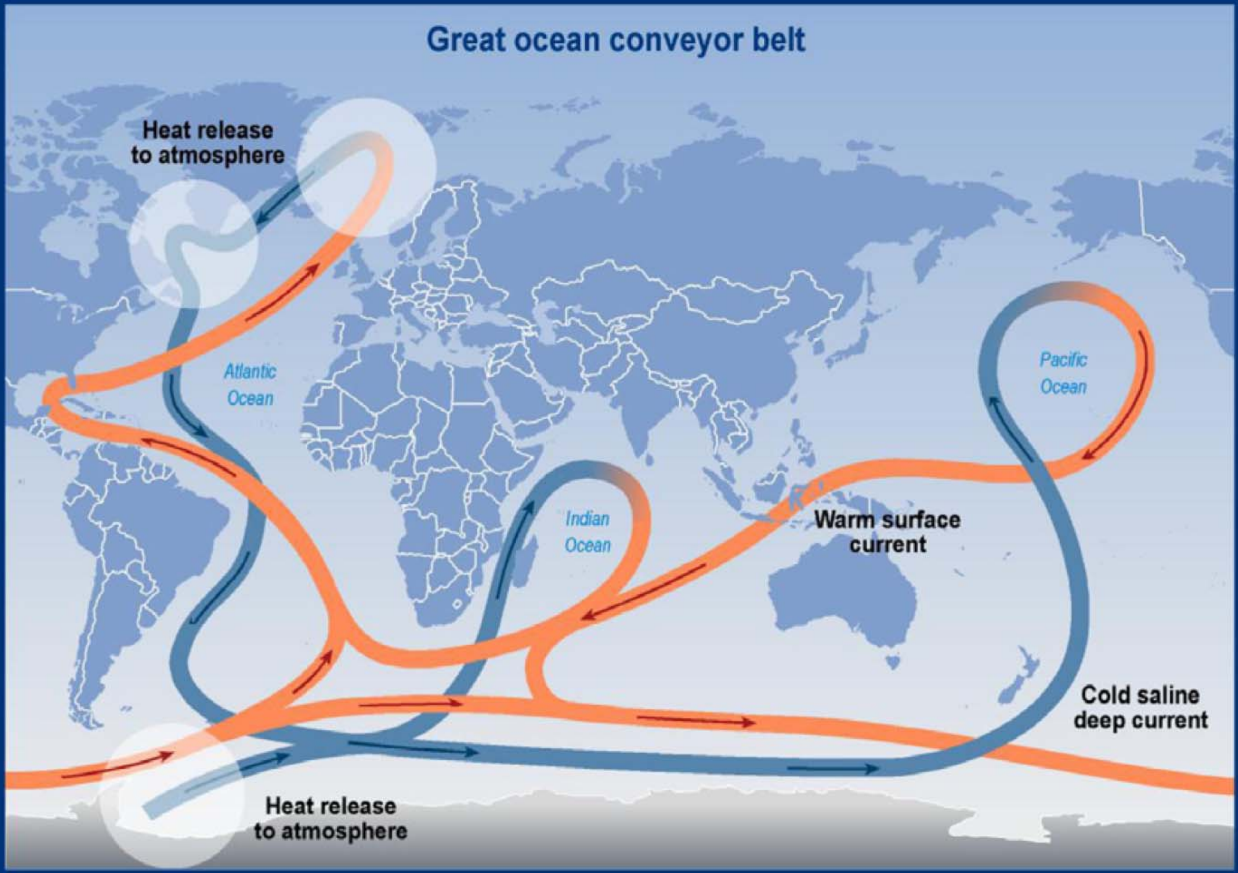

SYR - FIGURE 4-2

Superposition d'un mode interne thermohalin à la circulation forcée par le vent (Stommel, 1958)

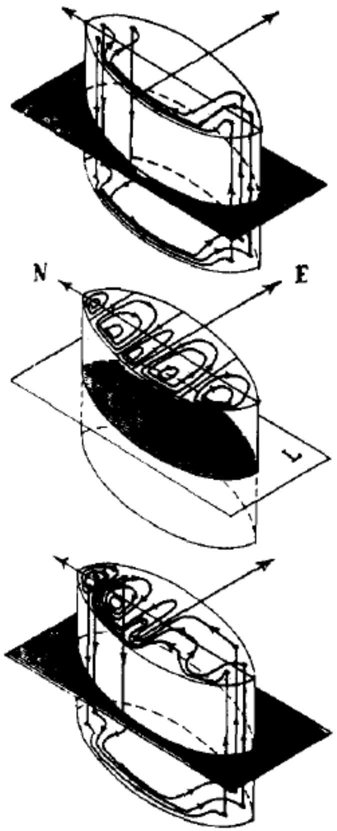

(a)

(b)

(c)

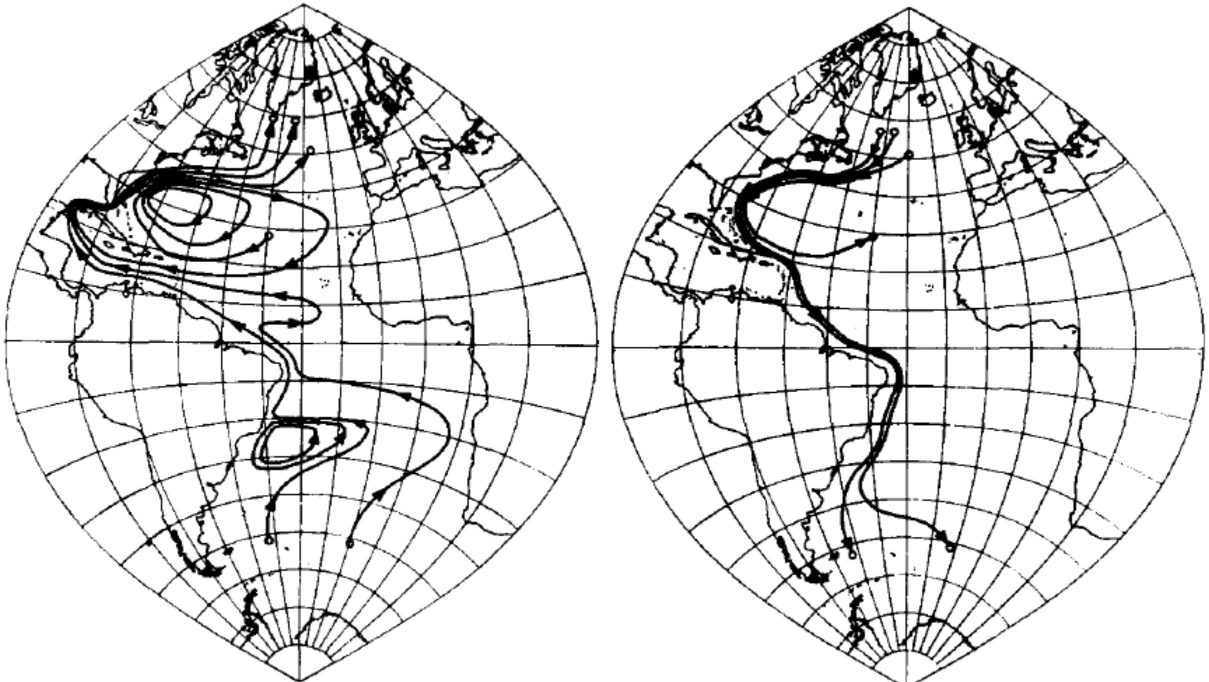

(a)

(b)

The future of the ocean conveyor belt

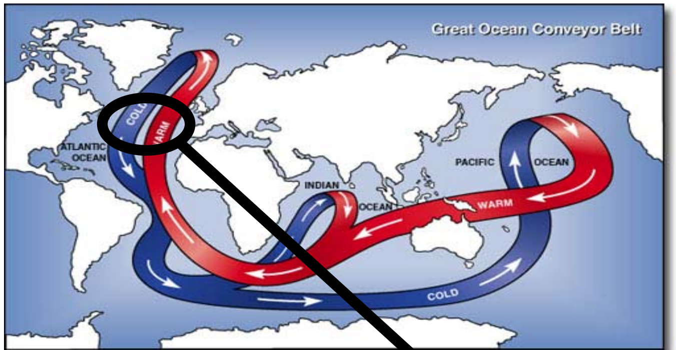

Schmittner et al. 2005

$1\ Sv = 10^6\ m^3\ s^{-1}$

Projection of the Atlantic meridional overturning circulation (MOC)

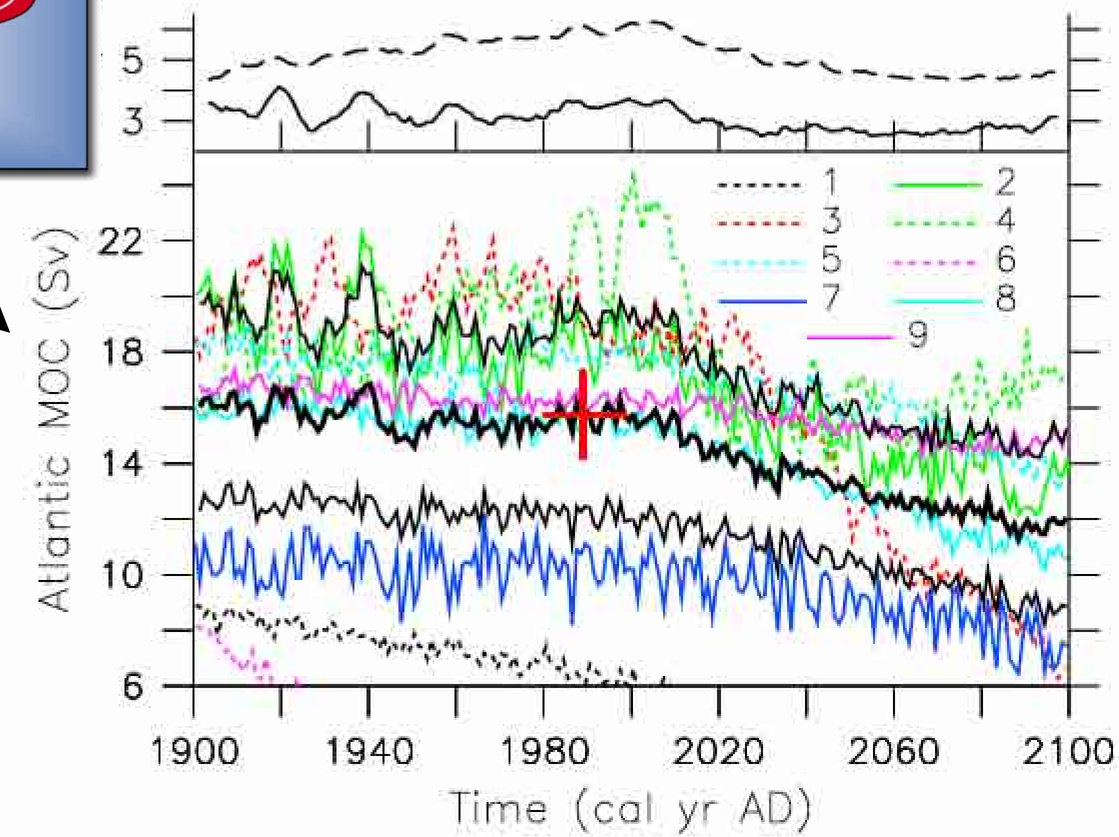

Slowing of the Atlantic meridional overturning circulation at 25° N

Harry L. Bryden[1], Hannah R. Longworth[1] & Stuart A. Cunningham[1]

Nature (2005)

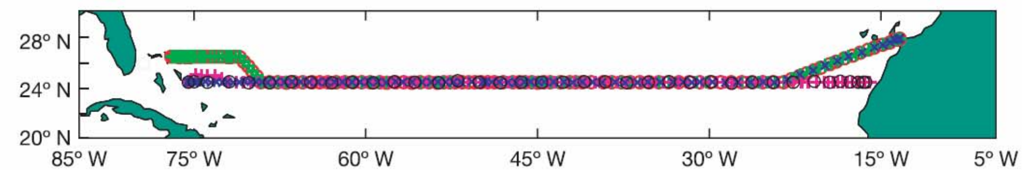

Figure 1 | Station positions for transatlantic hydrographic sections taken in 1957, 1981, 1992, 1998 and 2004. The 1957 and 1992 sections each went zonally along 24.5° N from the African coast to the Bahama Islands. Because of diplomatic clearance issues, the 1981, 1998 and 2004 sections angled southwestward from the African coast at about 28° N to join the 24.5° N section at about 23° W. The 1998 and 2004 sections angled northwestward at about 73° W to finish the section along 26.5° N.

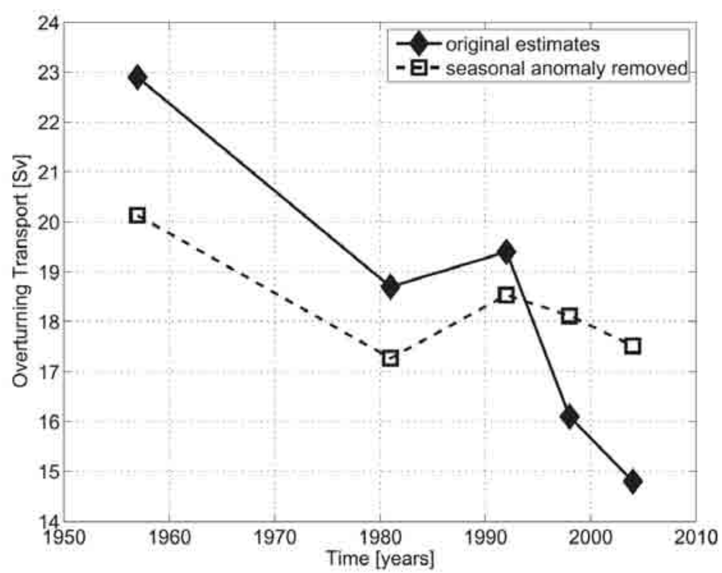

Erreur ~ 6 Sv

1 Sv 10^6 m^3 s^{-1}

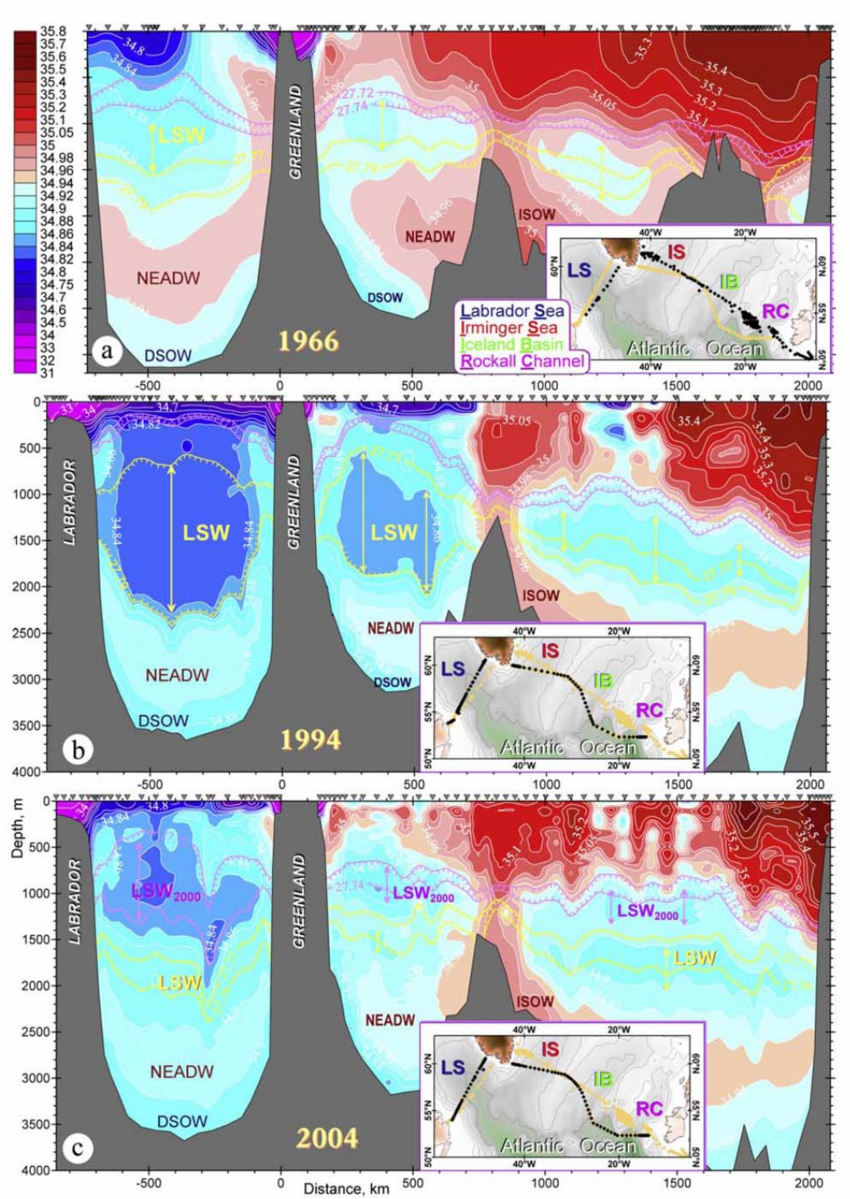

Figure 2

Variabilité de la convection profonde en mer du Labrador.

Yashayaev et al. (2007)

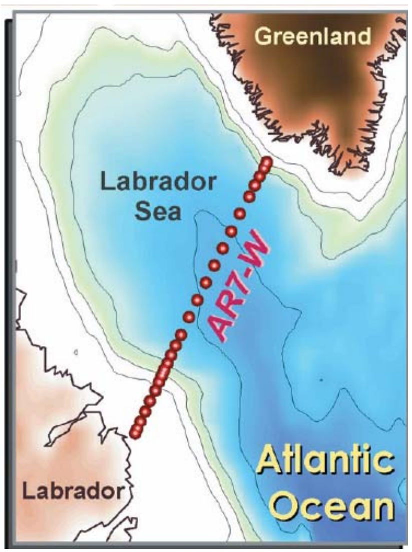

Yashayaev and Loder (2009)

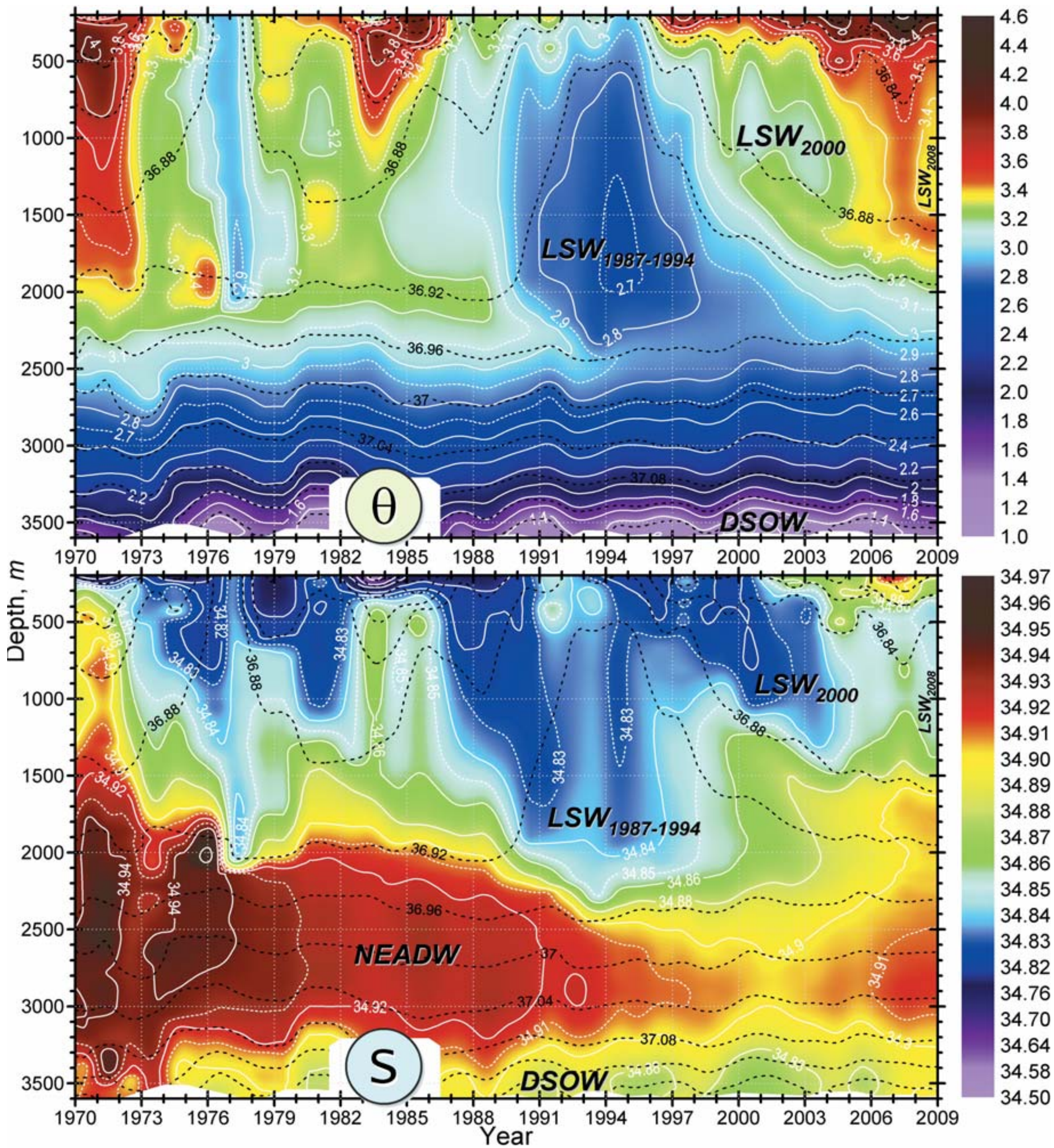

L'oscillation Nord Atlantique

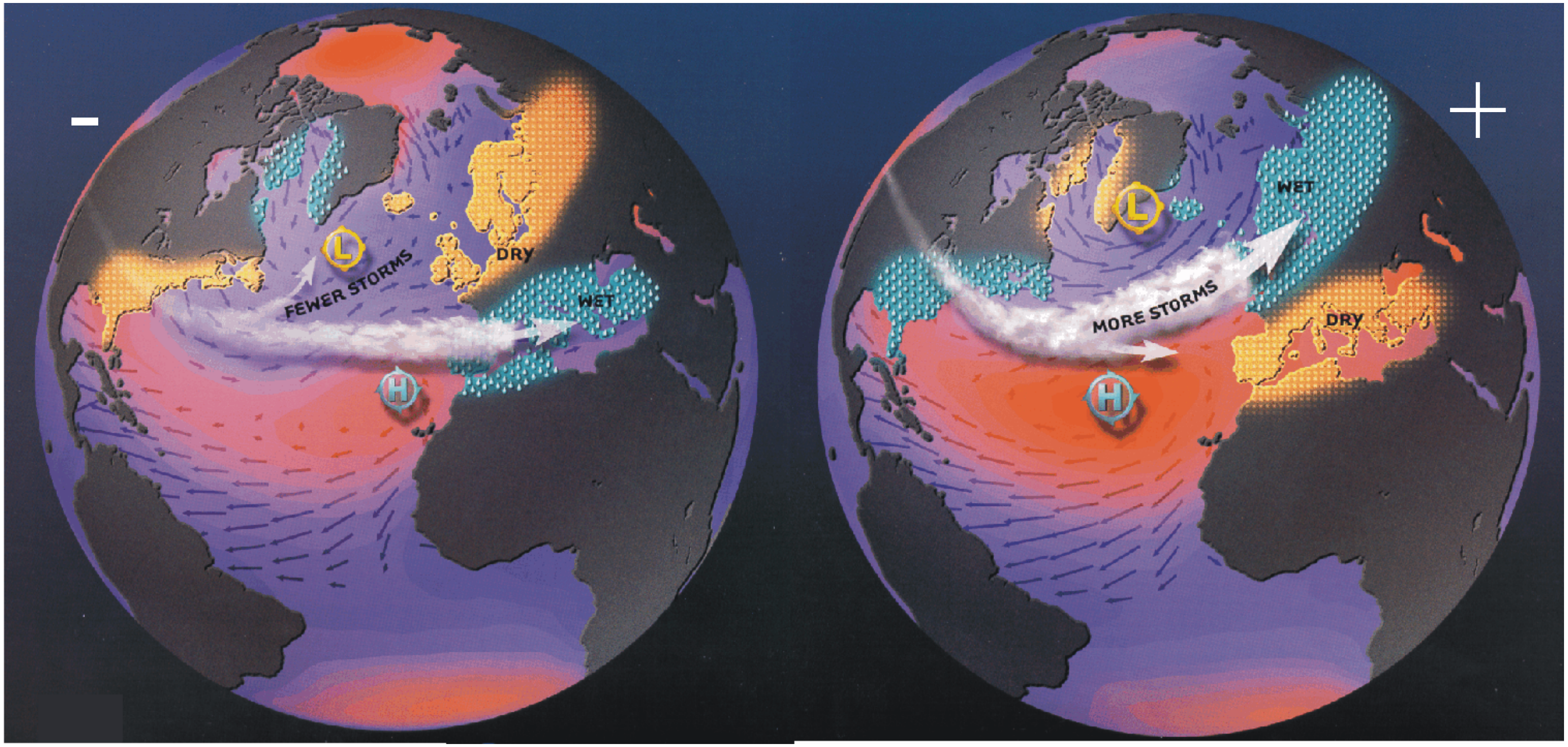

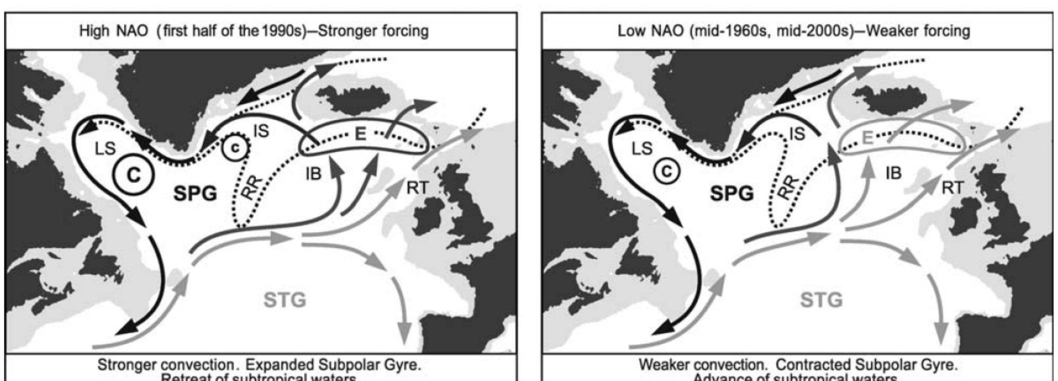

Sarafanov 2009

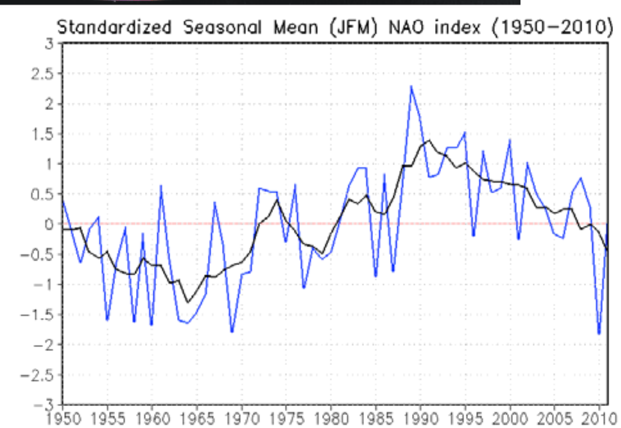

NOAA (2011)

Anomalies de la cellule méridienne de retournement (MOC) dans un modèle à haute résolution spatiale (Boening et al. 2005)

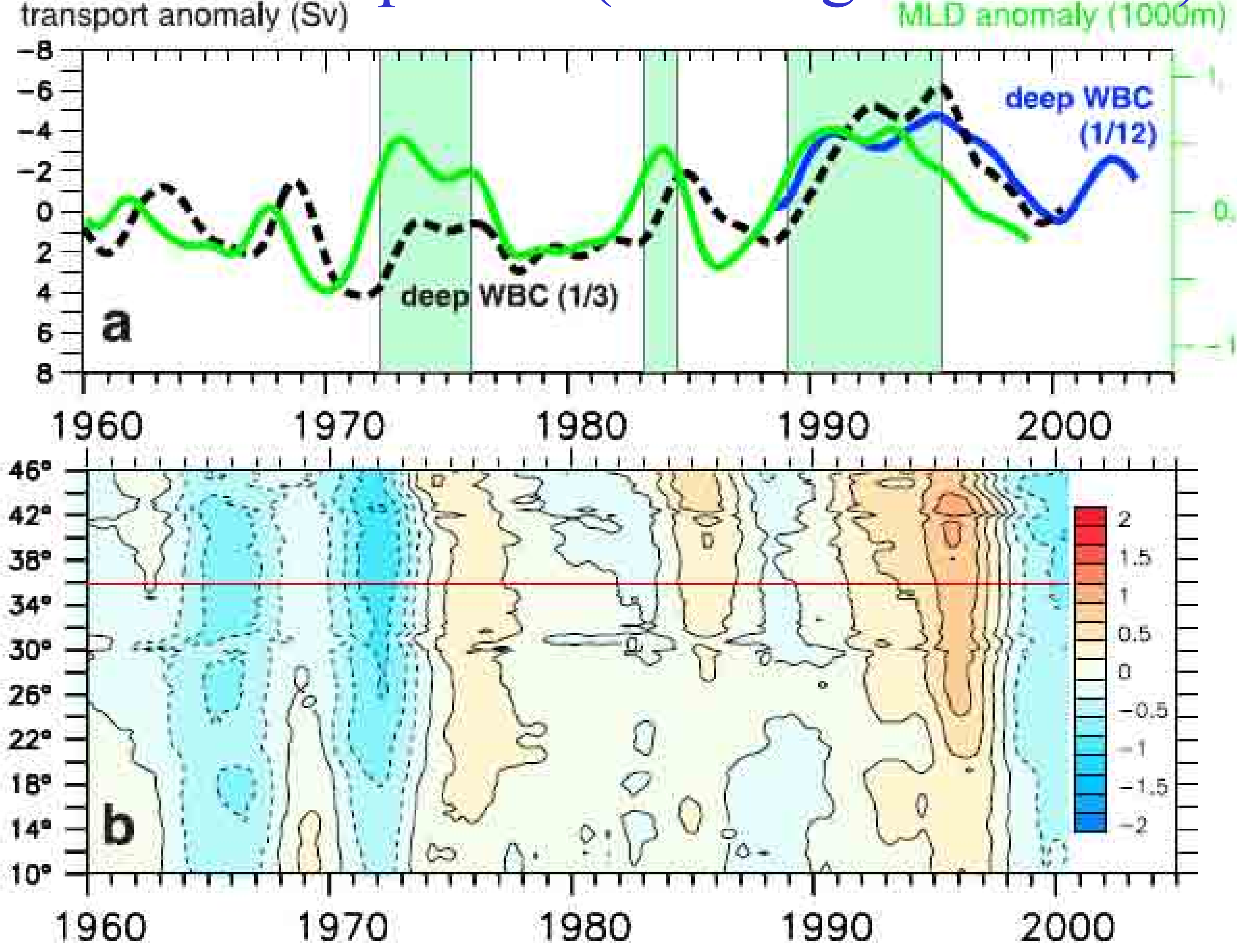

Towards a MOC index at subpolar latitudes from sustained measurements ?

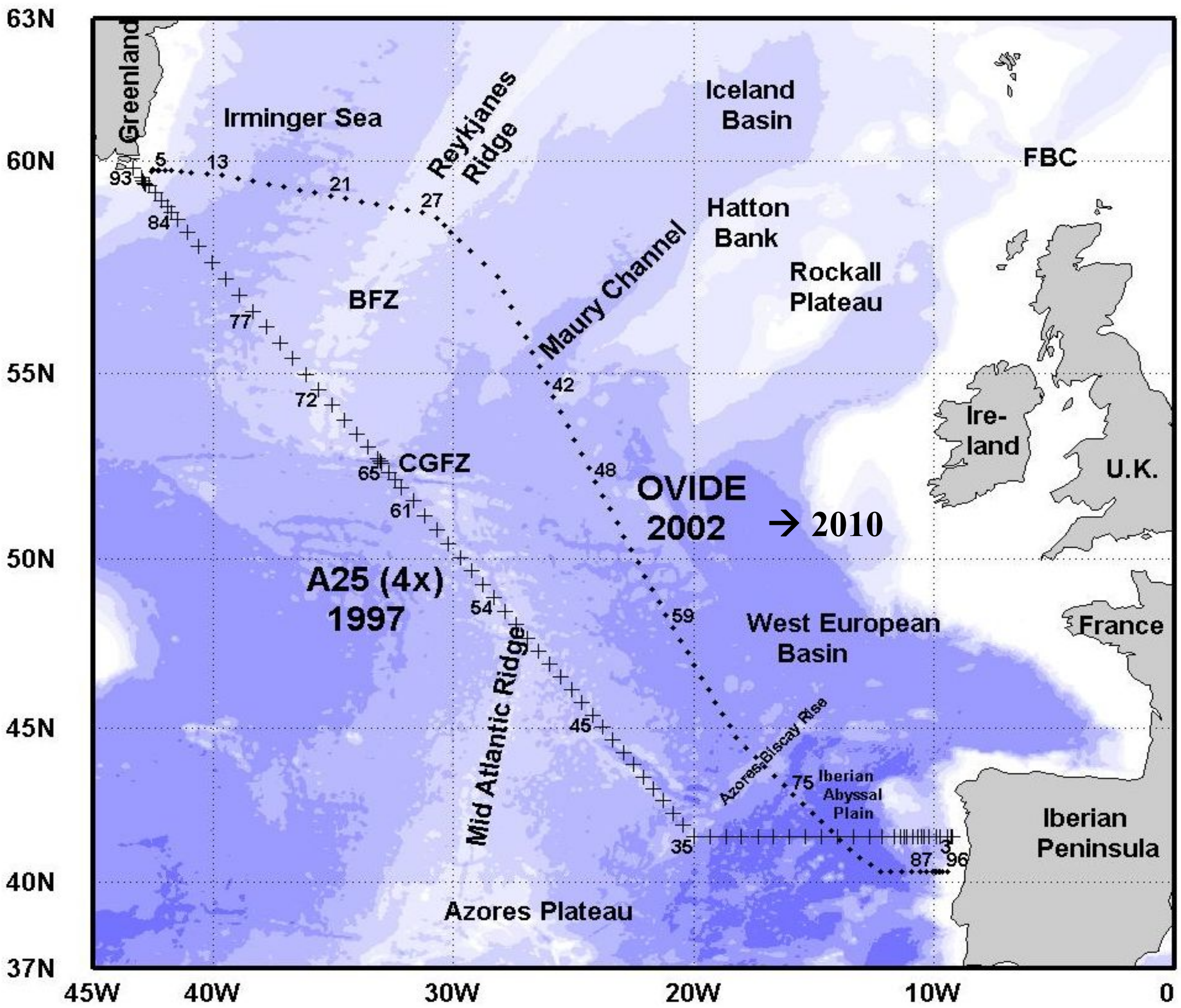

Circulation scheme across and North of the A25-OVIDE section

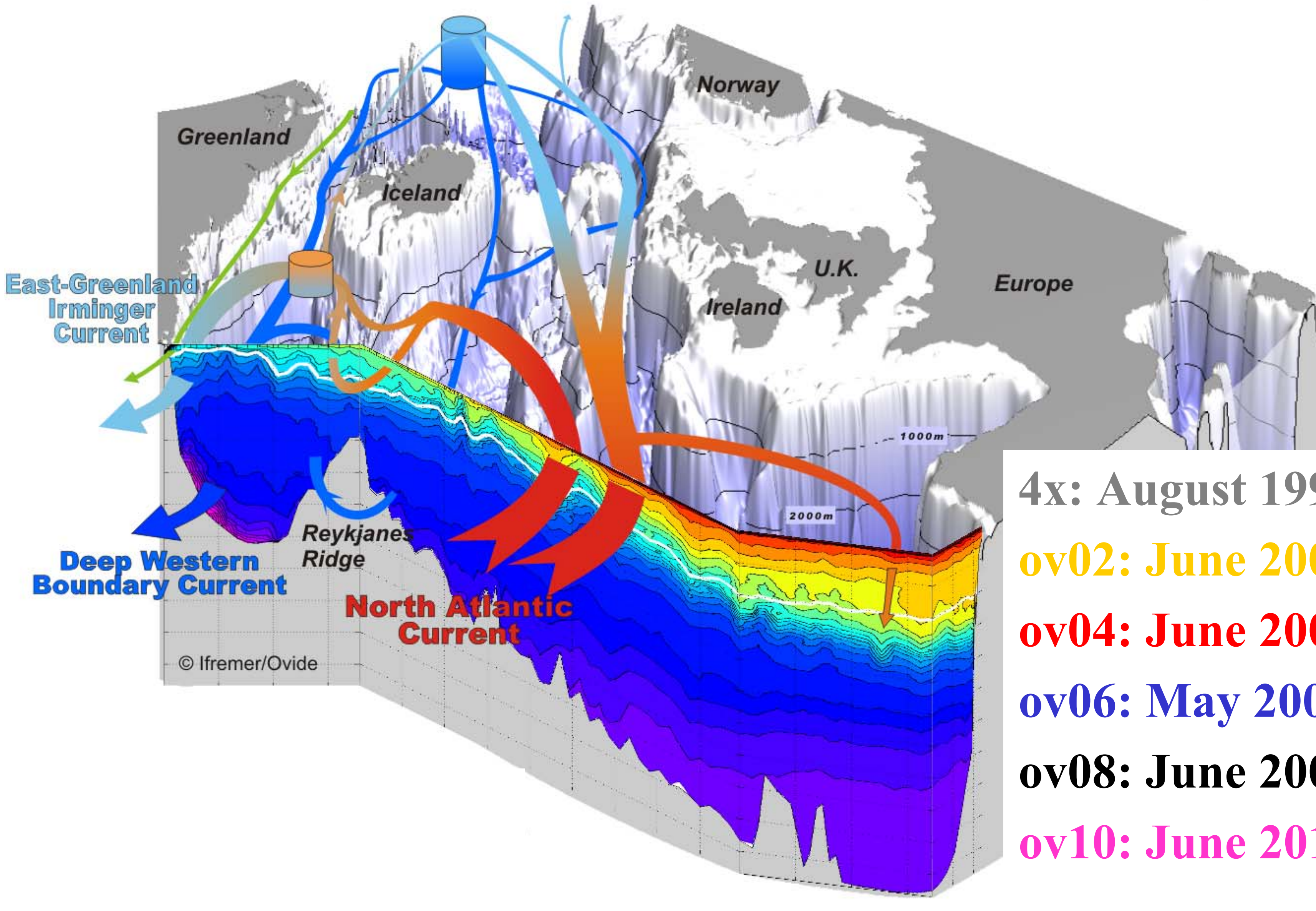

4x: August 1997
ov02: June 2002
ov04: June 2004
ov06: May 2006
ov08: June 2008
ov10: June 2010

L'observation du champ de densité ne donne accès qu'au cisaillement vertical des vitesses géostrophiques perpendiculaires aux stations hydrologiques

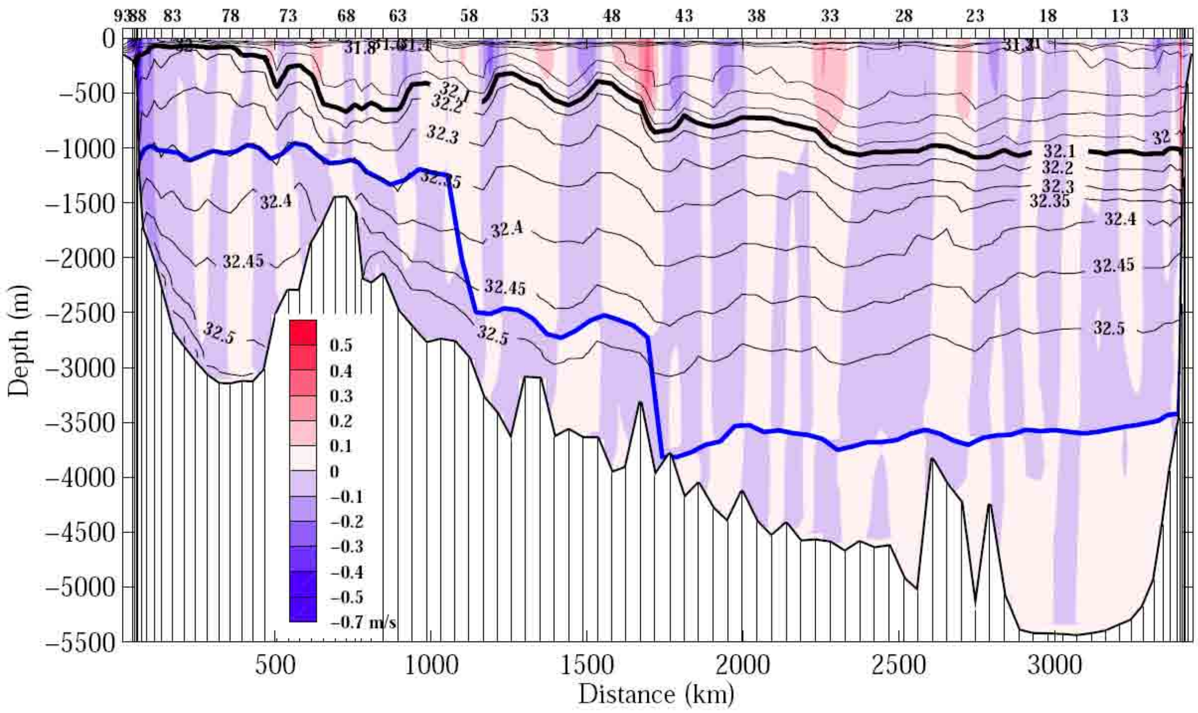

Velocity field for OVIDE 2010

Before inversion

Method for absolute transport estimation

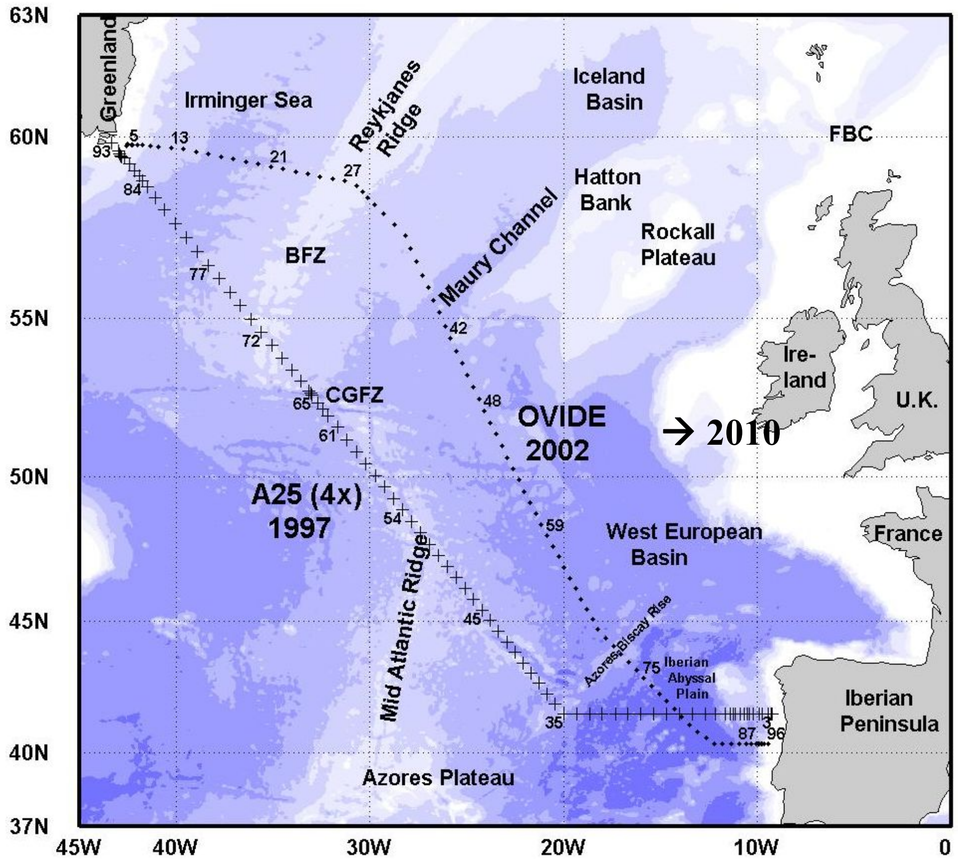

The absolute transports perpendicular to the section were estimated ***for the month of the cruise*** using a geostrophic inverse model that combines hydrography and ship-mounted ADCP measurements under an overall mass balance constraint (Lherminier et al. 2007)

SADCP data

SADCP data are quite reliable:

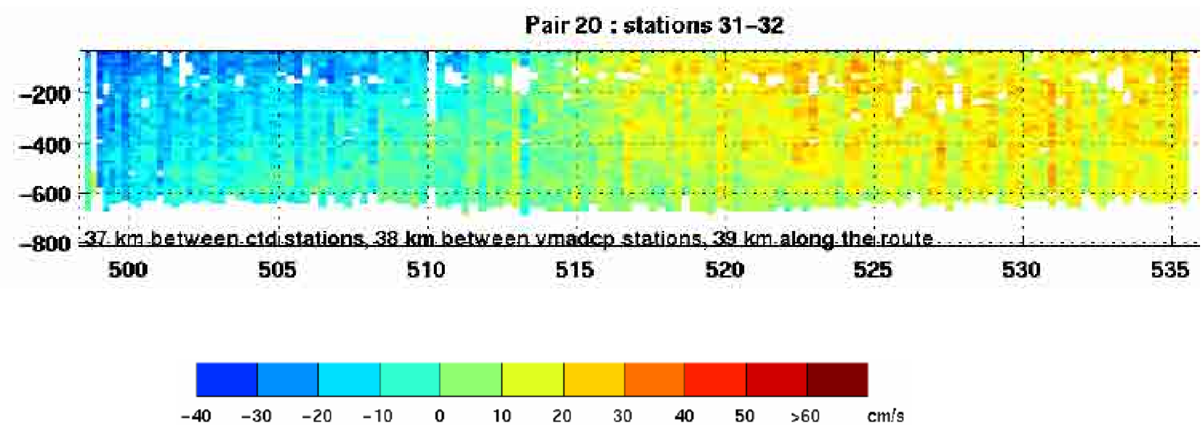

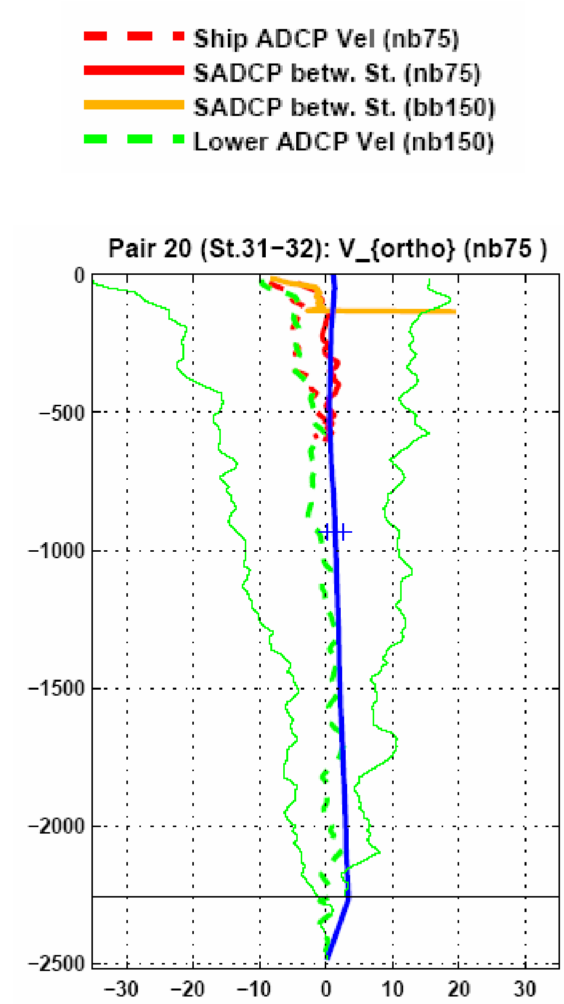

Pair 20 ADCP constraint:
+0.6 ± 2.2 cm/s
between 198 et 406m

Velocity field for OVIDE 2010

Before inversion

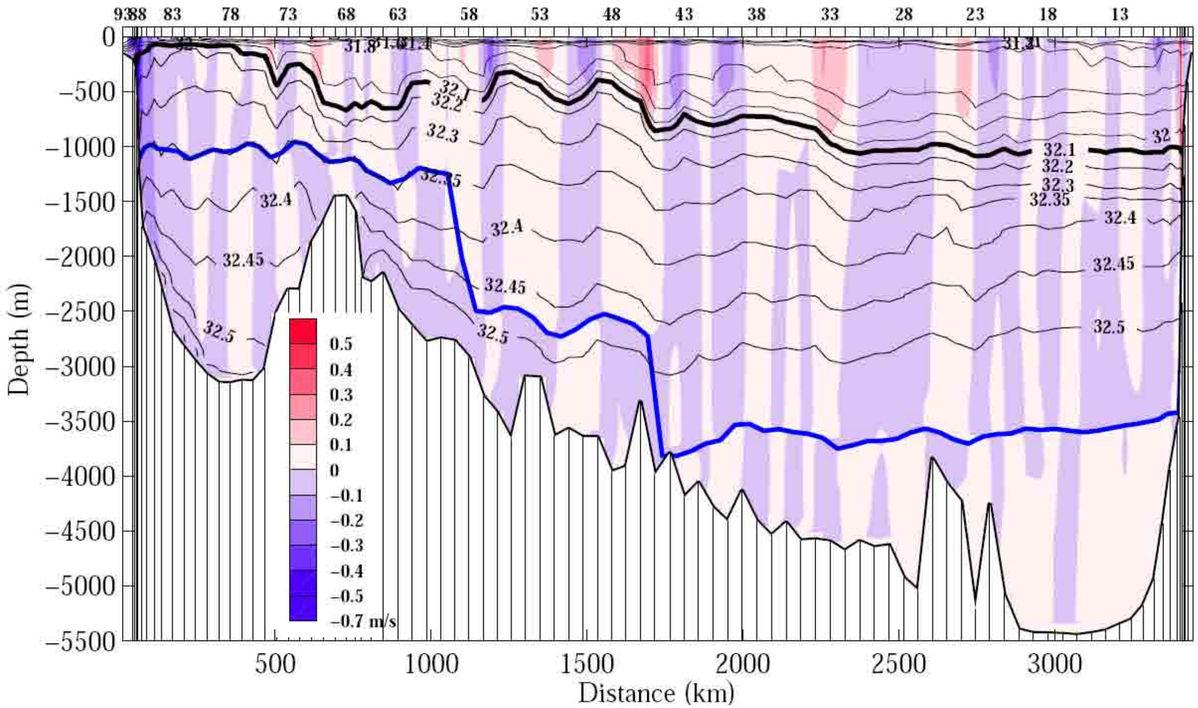

After inversion

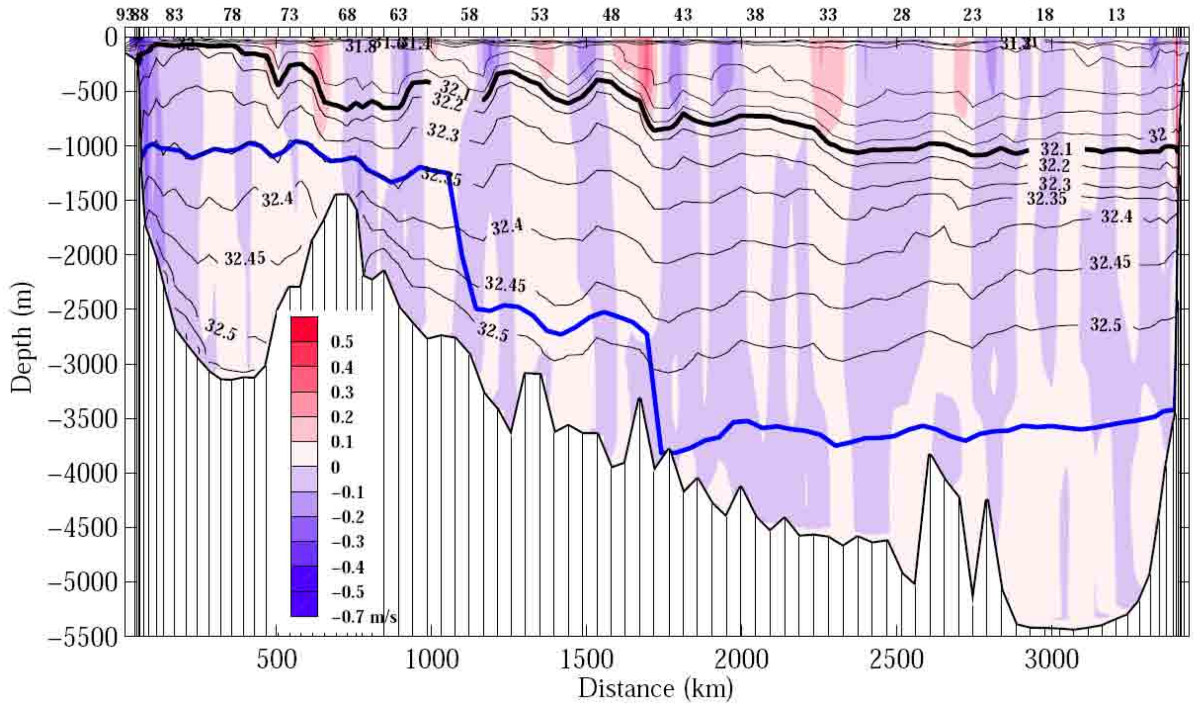

S-ADCP versus Altimetry constraints

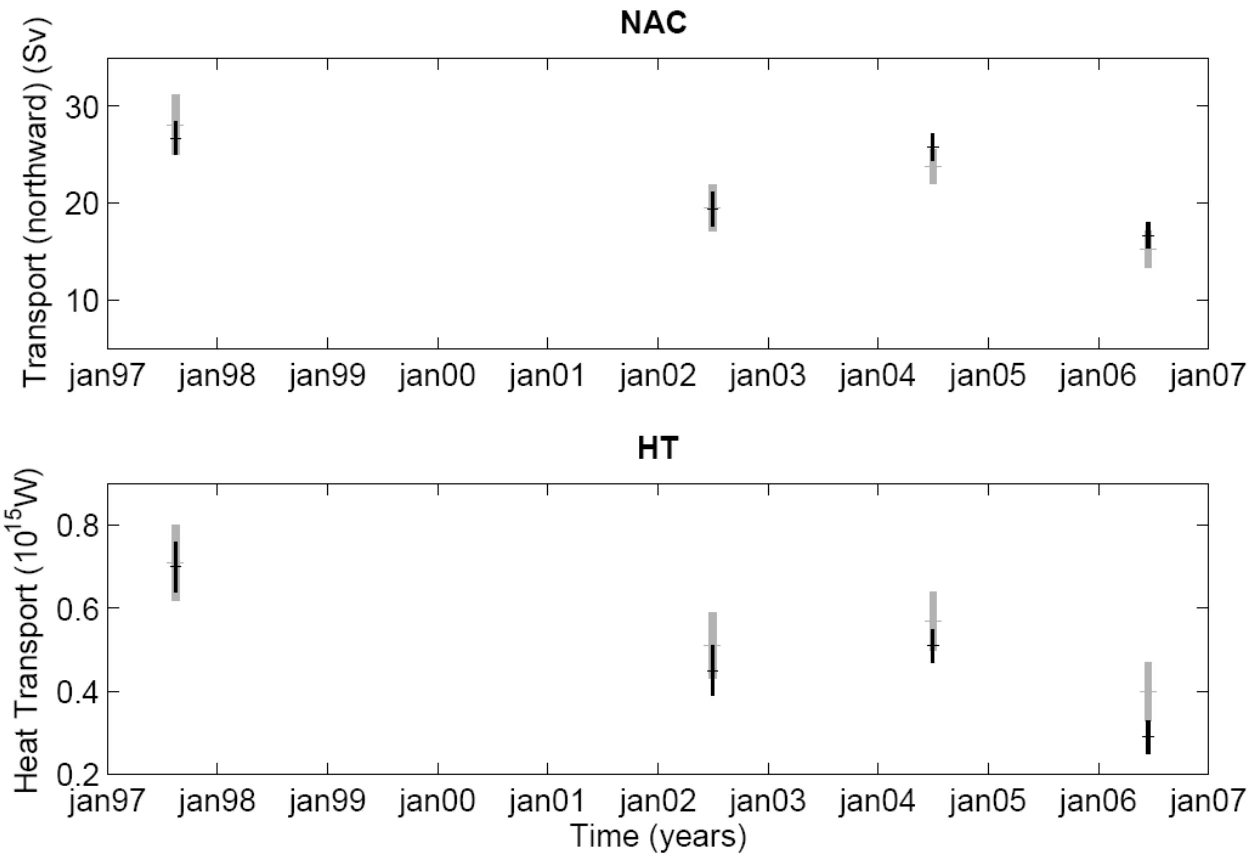

Altimetry constraints

S-ADCP constraints

Gourcuff et al. (JAOT, 2011)

Main components of the MOCσ

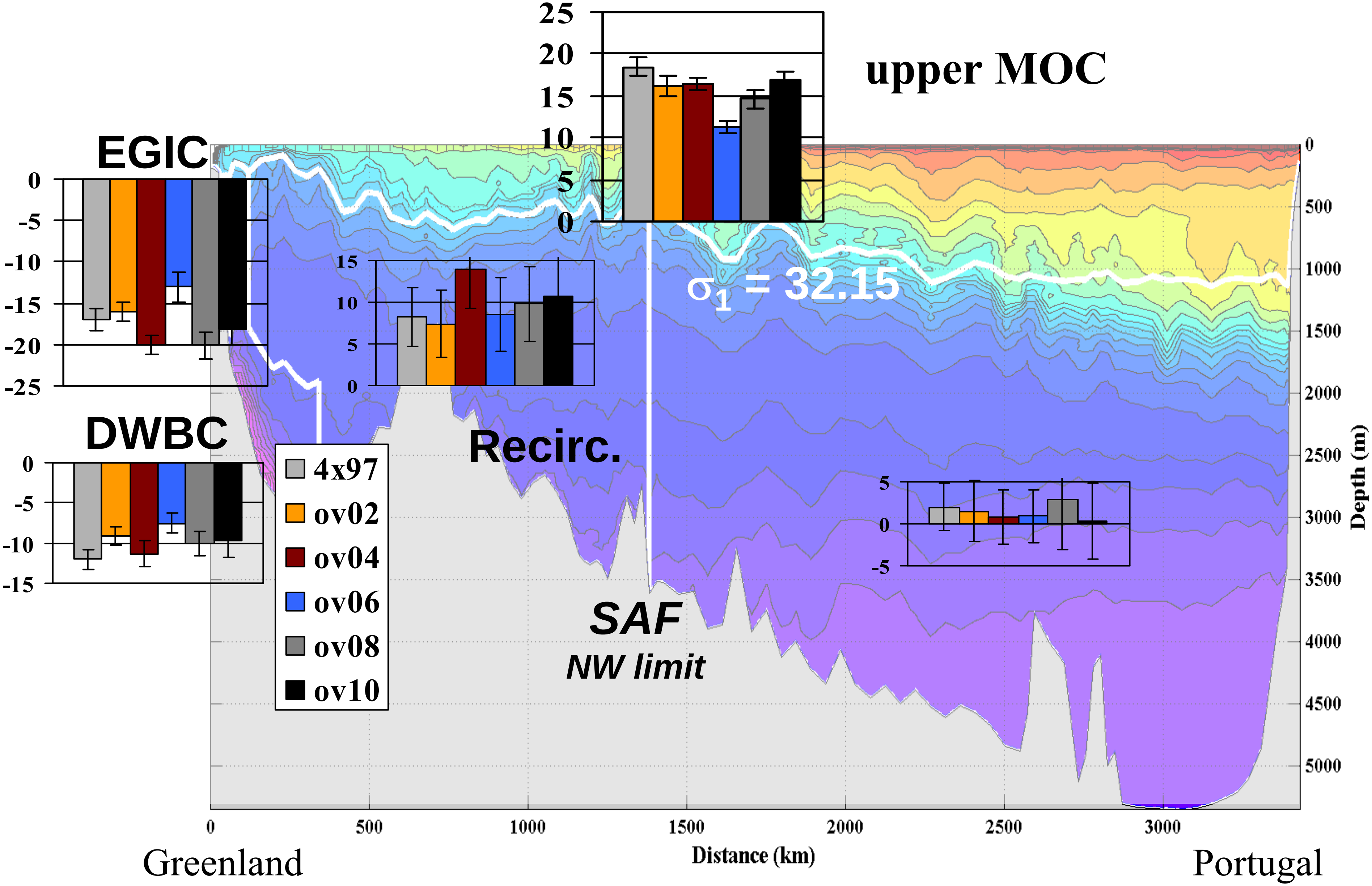

Comparison with transports from a current meter array in the EGIC

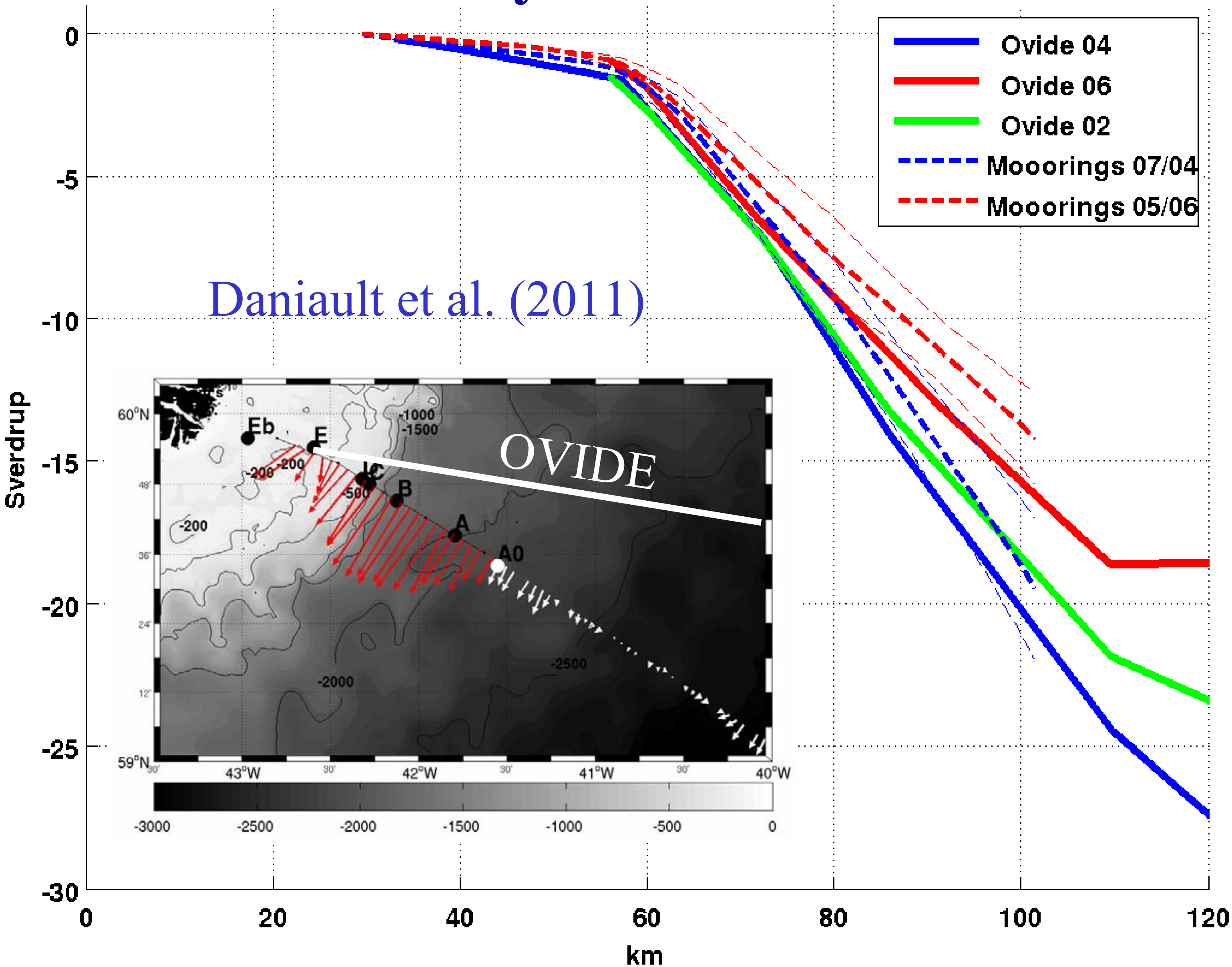

MOC$_\sigma$ transport variability

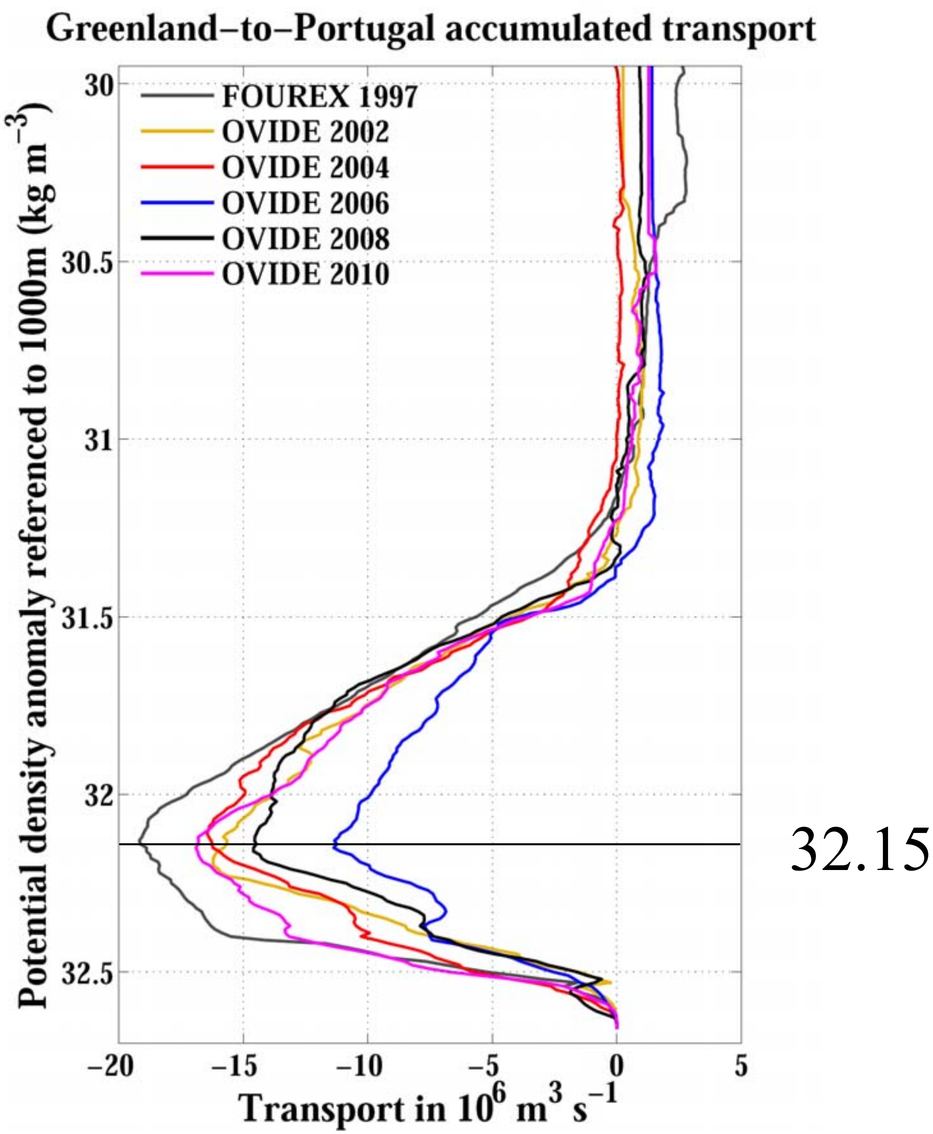

MOCσ	
4x97	18.5
ov02	16.2
ov04	16.4
ov06	11.2
ov08	14.6
ov10	16.8

MOC in Sv; error ~ 2 Sv

<MOC> = 15.6 Sv

A monthly MOC index from altimetry and Argo

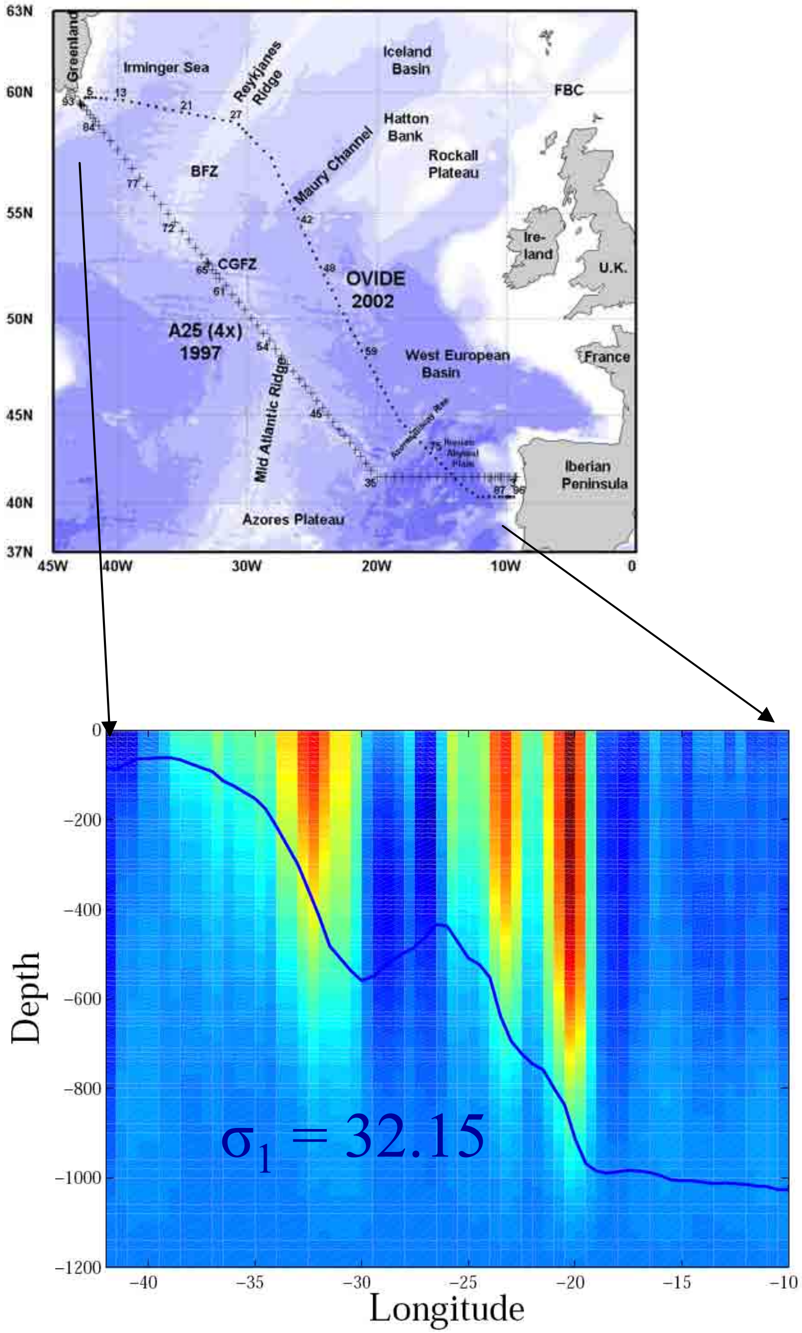

- Geostrophic velocities referenced to the surface are computed from the ISAS mapped Argo T, S fields (F. Gaillard, LPO)

- Absolute surface velocities are from the AVISO mapped altimetry products

- The MOC index is the transport above σ_1 = 32.15 (available every month)

A monthly MOC index from altimetry and Argo

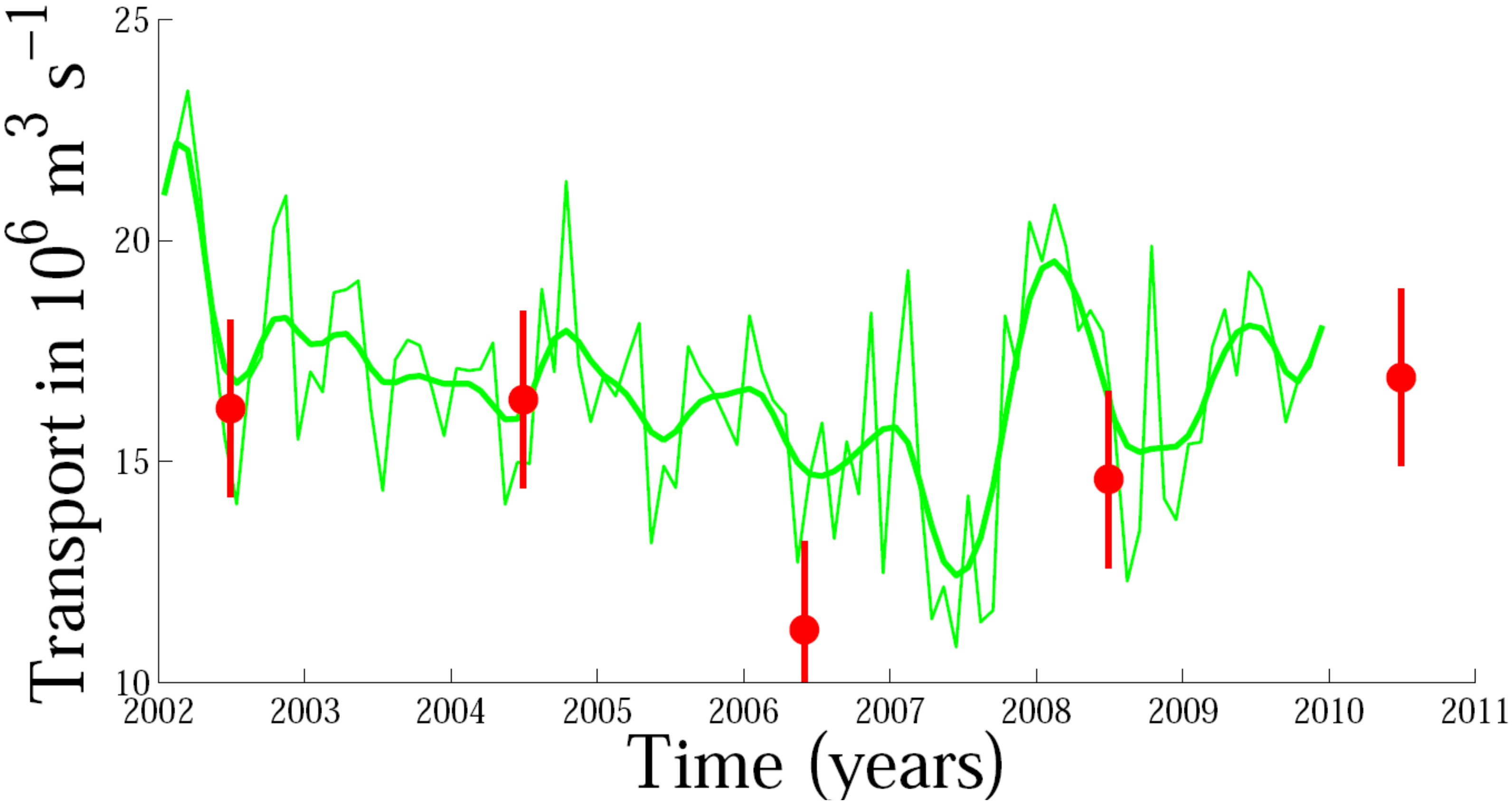

A MOC index from altimetry only

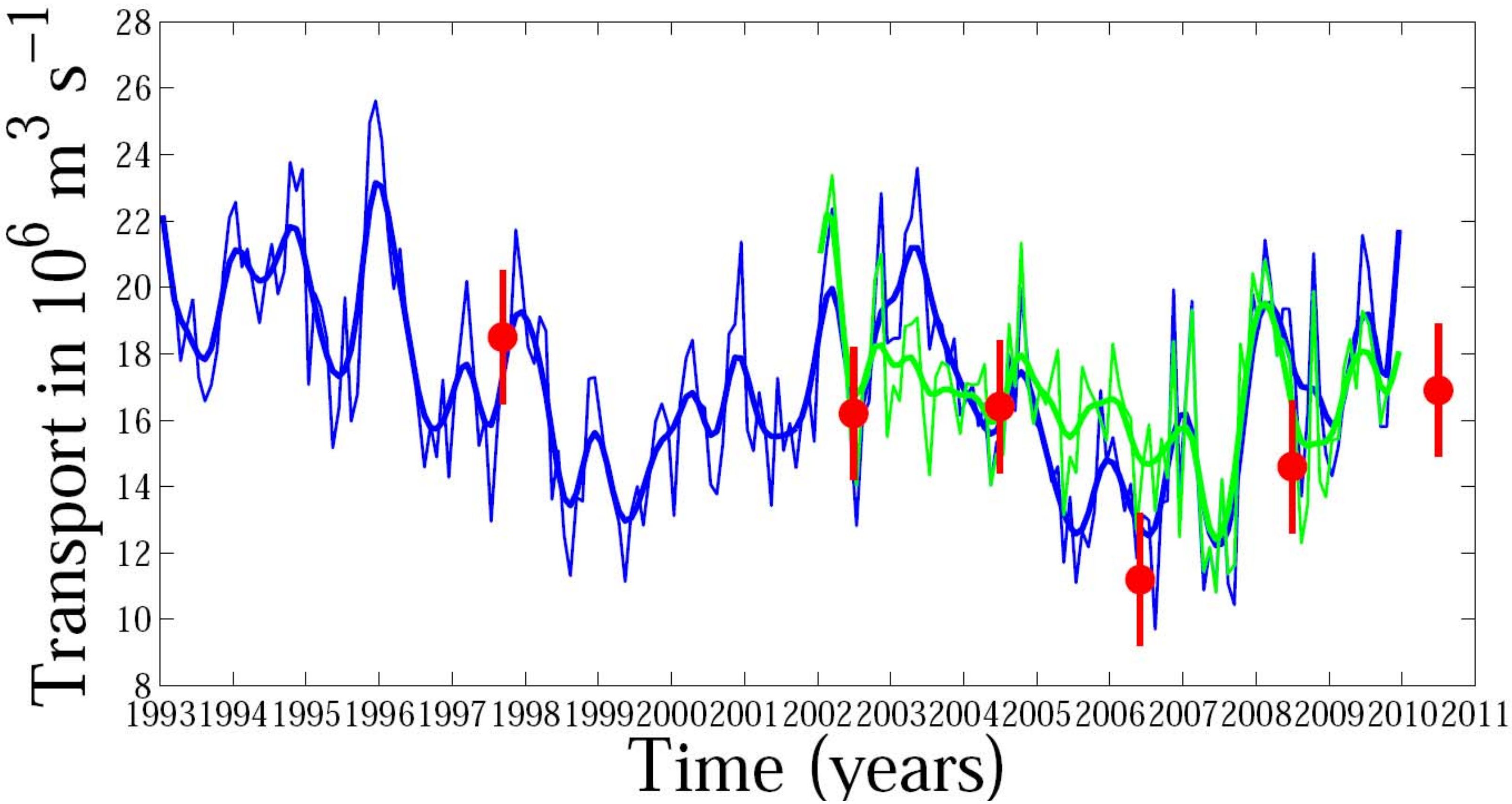

Linear trend : decline of 2 Sv since the mid 1990's

Relation avec la variabilité de la circulation de surface ?

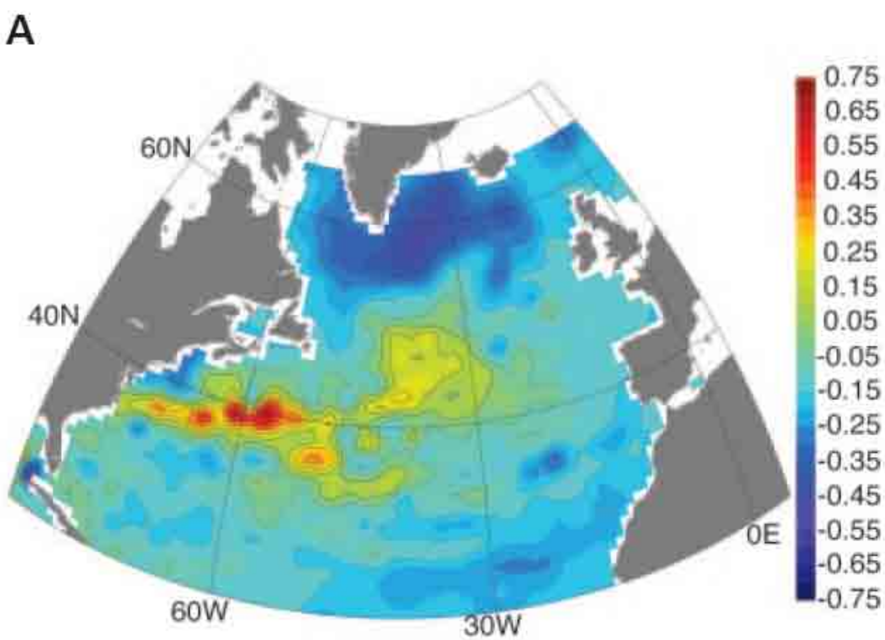

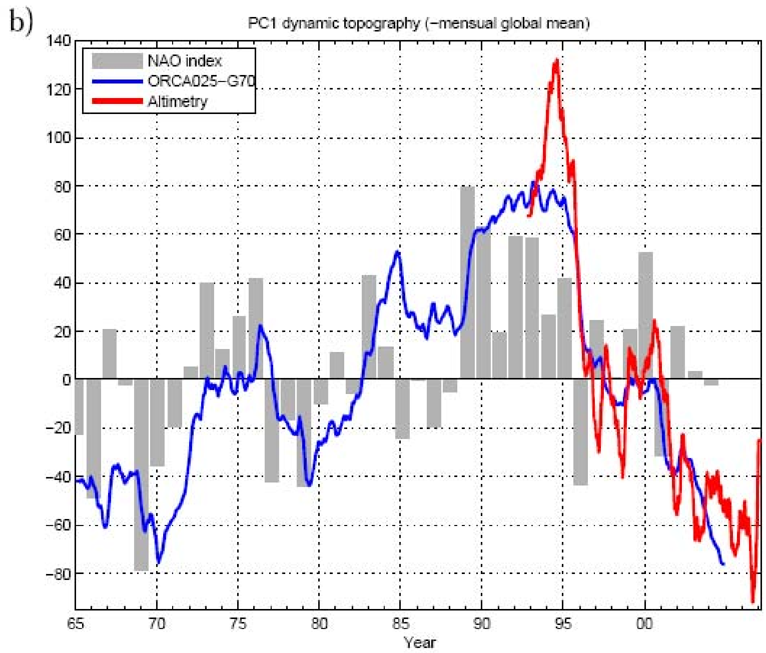

Adapted from Hakkinen and Rhines (2004)

Main components of the MOCσ

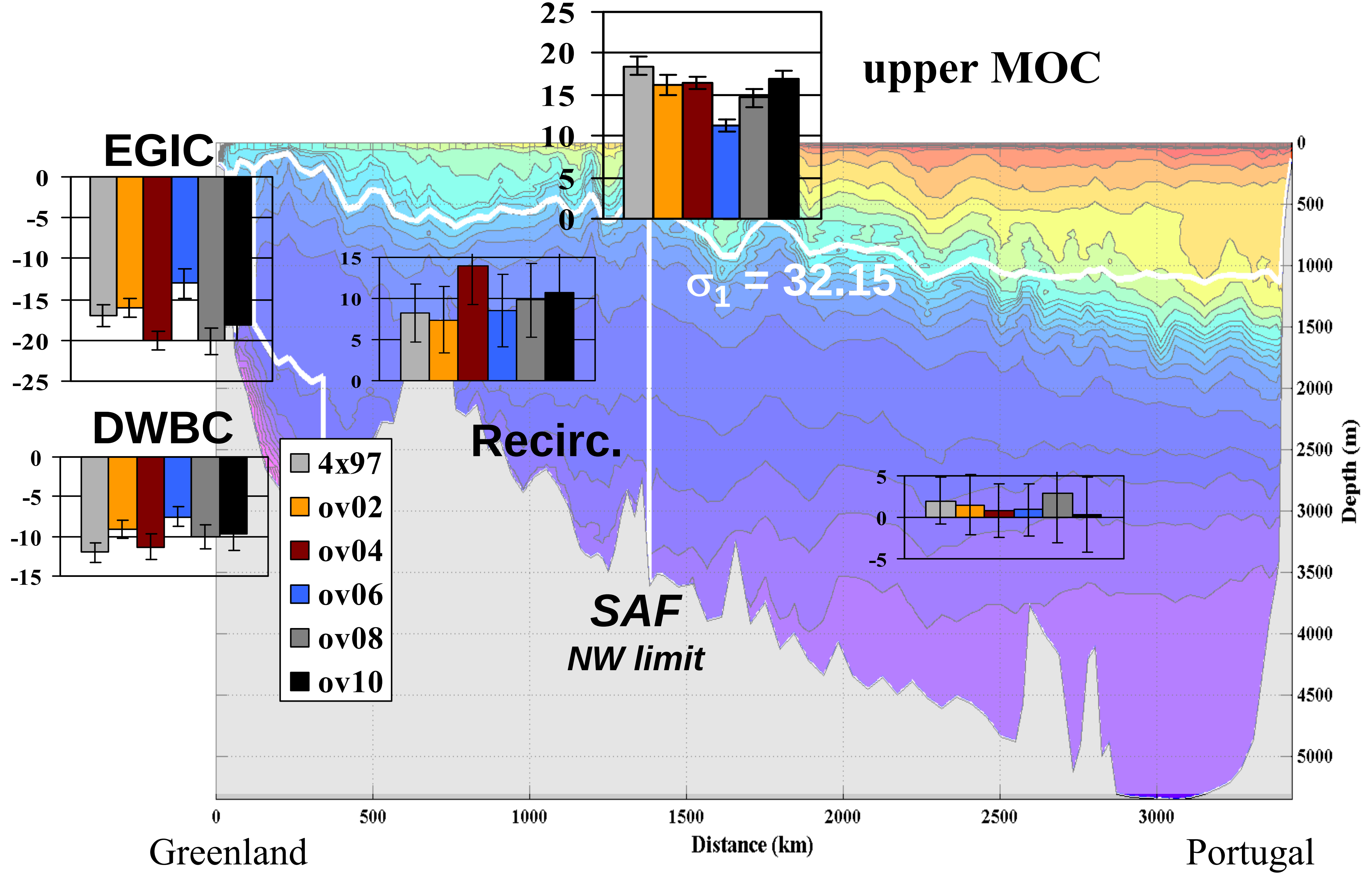

MOC_σ and heat transport variability

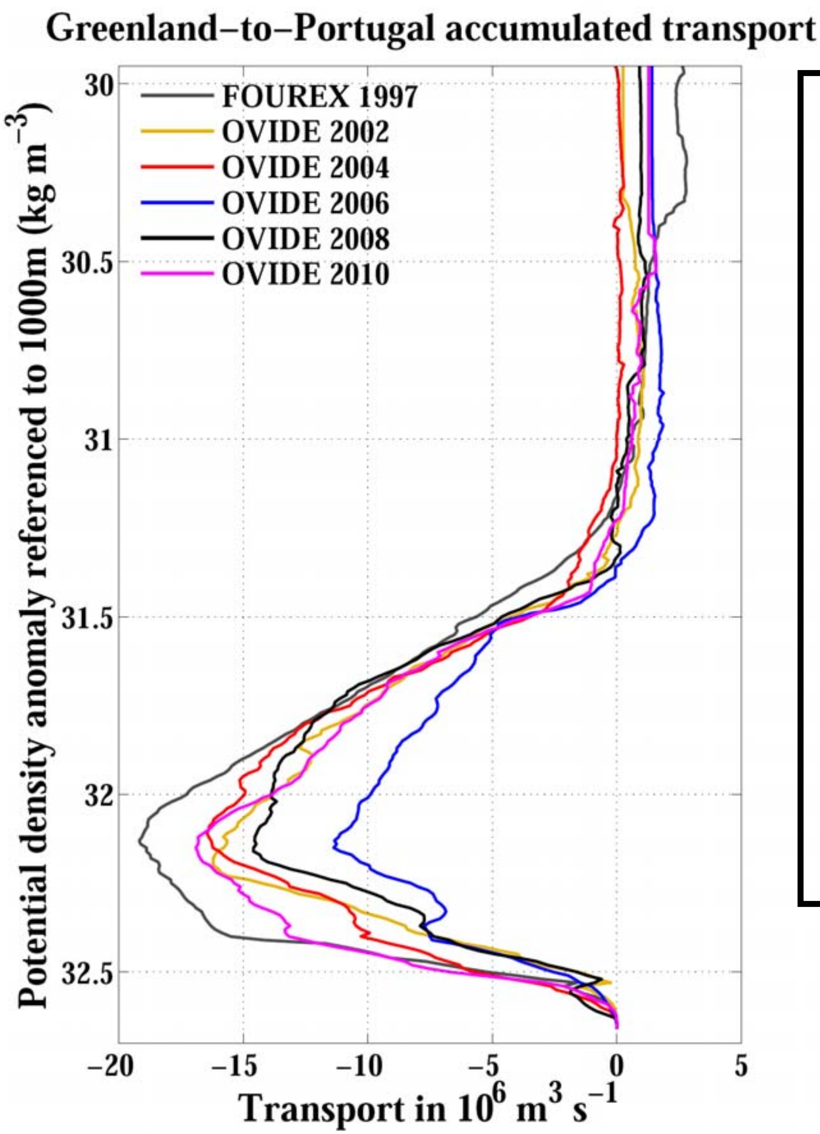

	MOCσ	HF	HF_{MOC}	HFiso
4x97	18.5	0.69	0.64	0.05
ov02	16.2	0.44	0.41	0.03
ov04	16.4	0.50	0.42	0.08
ov06	11.2	0.29	0.33	-0.04
ov08	14.6	0.47	0.42	0.04
ov10	16.8	0.58	0.51	0.07

MOC in Sv; error ~ 2 Sv

HF in PW; error ~ 0.05 PW

<HF> = 0.45 PW

Evolution du contenu thermique au nord de la section OVIDE

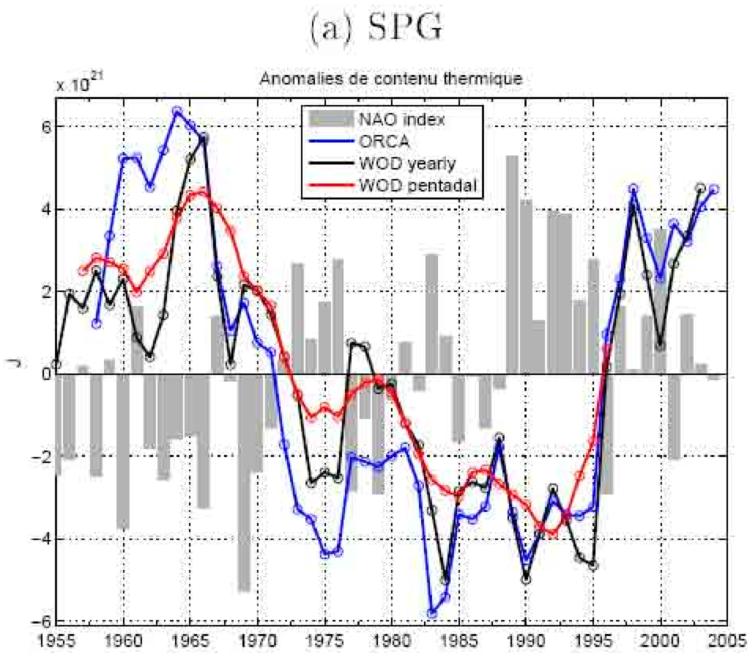

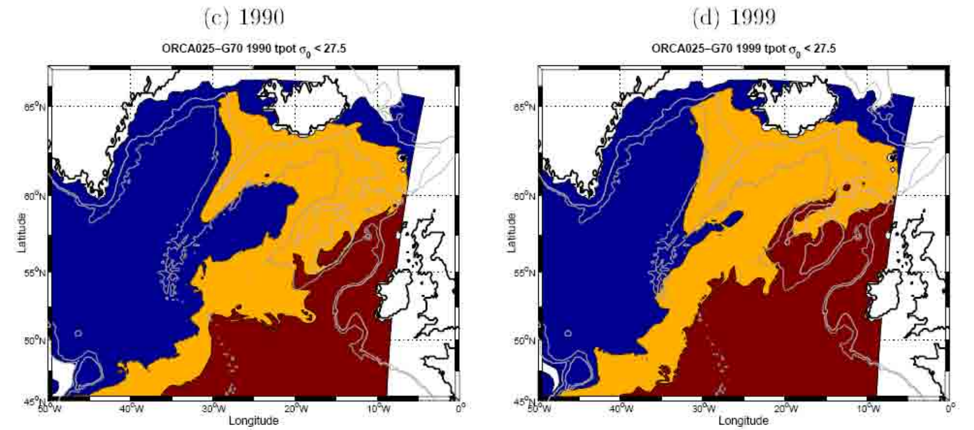

De Boisséson et al. (2011), Hatun et al. (2005)

Evolution du contenu thermique au nord de la section OVIDE

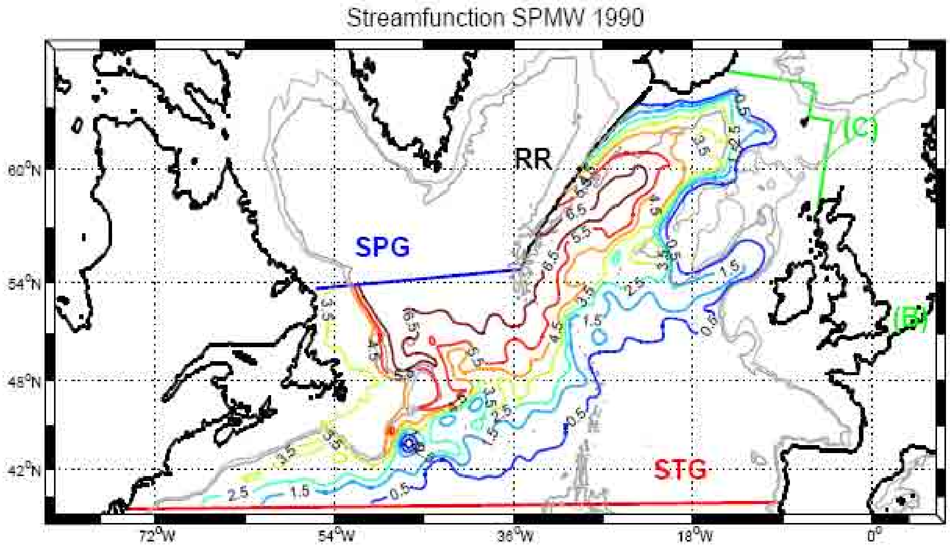

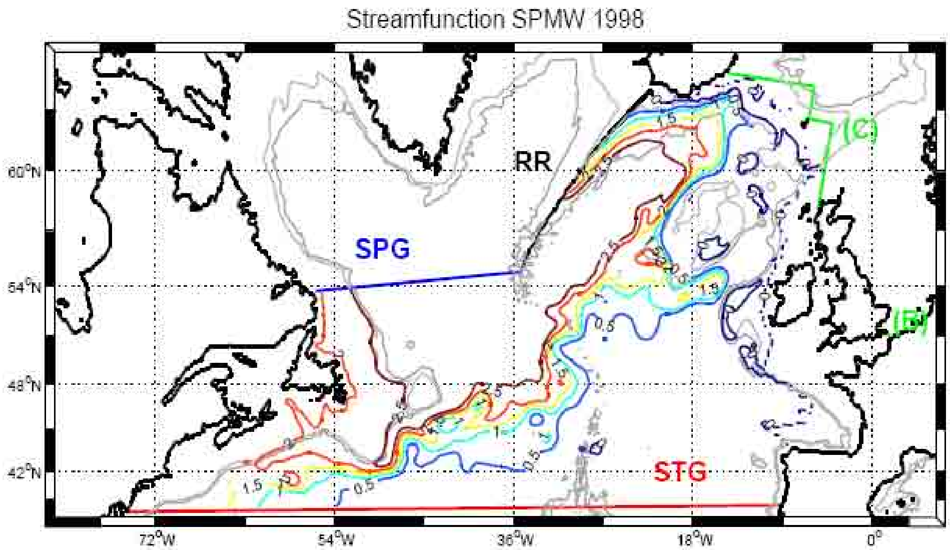

- L'advection des eaux d'origine subtropicale domine celle des eaux subpolaires en période NAO-

-Les pertes de chaleur du gyre subpolaire plus faible en période NAO – qu'en période NAO +

de Boisséson et al. (2011)

Desbruyères et al. (2011)

Conclusions

- A decomposition based on in situ observations, allowed the derivation of a MOCσ index from Argo and Altimetry, compatible with hydrographic estimates and varying in the range 12-23 Sv. An energetic low-frequency variability (~ 8-9 years) is evidenced from the 1993-2009 MOC index (altimetry only). Useful benchmark for numerical models.

- A MOC decrease of 2Sv evidenced between 1995-2009 might be linked to NAO (decrease in convection intensity and surface circulation). Will it propagate southward ?

- What are the consequences in term of heat content variability North of Ovide Section ? Does the Labrador Sea matter ?